12WCEE 2000

STRESS DROP AND FMAX ESTIMATED FROM STRONG MOTION RECORDS OBSERVED AT DEEP BOREHOLES IN JAPAN

Toshimi SATOH[1], Yoshihisa KOBAYASHI[2] And Hiroshi KAWANO[3]

SUMMARY

In this study we examine the relation between *fmax* and seismic moment and the relation between *fmax* and stress drop in order to quantitatively evaluate spectral amplitudes in the high frequency range. We use horizontal components of strong motion records observed by accelerometers installed at GL-330 m in Iwaki and at GL-950 m in Tomioka, Japan. The JMA magnitudes of 50 earthquakes range from 4.0 to 6.6 and the epicentral distances range from 22 to 150 km. Stress drop $\Delta\sigma$, *fmax*, and seismic moment M_0 are estimated to fit observed spectrum to the model spectrum based on ω^{-2} model [Boore, 1983] in the frequency range less than 25 Hz. As a result it is shown that *fmax* has no correlation with M_0. On the other hand we obtained

$\log \Delta\sigma = -2.91 \log fmax + 5.8$ (σ=0.296 ; σ is standard deviation)

by a regression analysis using strong motion records of 30 earthquakes occurred off Fukushima prefecture in latitude about 37 ^{o} N (region-A, -B, and -C). This empirical relation suggests that *fmax* is source-controlled. We also show that the relation that $\Delta\sigma$ is nearly proportional to $fmax^{-3}$ is appreciable to 20 earthquakes occurred in the three other source regions nearby the region-A, -B, and -C, although absolute value of $\Delta\sigma$ varies with source regions. It is also found that the regression relation can explain *fmax*-$\Delta\sigma$ distributions estimated from subduction earthquakes occurred in latitude 37^{o} N to 40 ^{o} N in a previous study [Satoh et al., 1997]. In addition by substituting the regression relation into the source spectral model, we show that the spectral amplitude in the frequency range higher than *fmax* is independent on $\Delta\sigma$ and is scaled by only M_0.

INTRODUCTION

It is important for aseismic design for short-period structures such as nuclear power plants to quantitatively evaluate spectral amplitudes of strong motions in the high frequency range. The high-frequency Fourier spectra can be modeled by two parameters, that is, stress drop and high-frequency cutoff *fmax* [Hanks, 1982]. Although it has been a controversial issue whether *fmax* is source-controlled or site-controlled, the importance of effects of *fmax* on high-frequency spectra has been recognized. However, it is very difficult to estimate these parameters, especially *fmax*, from strong motion records because high-frequency spectra are easily affected by site amplifications due to very shallow subsurface layers even if seismometers are installed on so-called rock [e.g., Satoh et al., 1998].

Therefore in this paper we estimate *fmax* and stress drop from deep borehole records on which the effects of site amplifications are negligibly small. So far Hauksson et al. [1987] suggested the existence of site-controlled *fmax* using deep borehole records of a small earthquake with magnitude of 2.8 occurred in California. In Japan Kinoshita [1992] showed that *fmax* varies with source regions using deep borehole records of many earthquakes occurred around Kanto district, Japan and suggested the existence of source-controlled *fmax*. Although several researchers show that *fmax* decreases with seismic moment M_0 [e.g., Faccioli, 1986], they use records observed

[1] *Ohsaki Research Institute, Fukoku-seimei, Chiyoda-ku, Tokyo, Japan. Email : toshimi@ori.shimz.co.jp*
[2] *Tokyo Electric Power Company, Tokyo, Japan*
[3] *Tokyo Electric Power Company, Tokyo, Japan*

at surface. So we examine the relation between *fmax* and M_0 as well as the dependence of *fmax* on source regions using deep borehole records observed at bedrock in Iwaki and Tomioka, Japan. Moreover we examine the relation between *fmax* and stress drop and discuss the scaling of spectral level in the frequency range higher than *fmax*.

DATA

Accelerometers are installed at bedrock with the S-wave velocity of 2.8 km/s at GL-330 m in Iwaki and at GL-950 m in Tomioka, Japan [Omote et al., 1984]. The sensors and the amplifiers have flat amplitudes up to 25 Hz and the sampling rate is 0.005 seconds. We select strong motion records commonly observed at the two sites on the condition that the epicentral distances are less than 150 km. The number of the selected earthquakes occurred in 1982 to 1996 is 50. The JMA magnitude M_J range from 4.0 to 6.6. The focal depths tend to be deeper to west due to subduction of the Pacific plate and range from 35 to 93 km. The minimum epicentral distance is 22 km. The locations of the epicenters and the two borehole sites are shown in Figure 1. The region-A, -B, and -C are classified because many earthquakes swarmed, while the region-N, -M, and -S are classified based on the relation between stress drop and *fmax* as mentioned later. The 18 earthquakes out of 22 whose Harvard CMT solutions are determined [Dziewonski, 1981] have typical focal mechanisms of interplate earthquakes in the shallow subduction zone, that is, the thrust faults.

We use S-wave portions with the duration of 6 sec for earthquakes with $M_J \varepsilon 5.8$ or $M_0 \varepsilon 5 \infty 10^{24}$ dyne-cm and 3 sec for the other smaller earthquakes. The geometrical average of two horizontal spectra whose signal-to-noise ratio is greater than three is used for the following analysis. Here we regard time windows before the P-wave arrival as noise. All Fourier spectra used in this study are smoothed by the Parzen window with the band width of $0.1f$ (f is frequency).

Since Kato et al. [1992] show the site amplification factor at GL-330 m in Iwaki is around unity based on the one-dimensional wave propagation theory with PS logging results and the spectral inversion method, we calculate the spectral ratios of Tomioka to Iwaki and averaged them over all the earthquakes as shown in Figure 1. The average spectral ratio cannot be regarded as unity, so we correct the each spectrum observed at Tomioka by dividing it by the average spectral ratio.

METHOD

Acceleration spectrum for S-wave *A(f)* can be modeled [Boore, 1983] as

$$A(f) = C \cdot M(f) P(f) \frac{T(f)}{X} Z(f) \cdot \quad (1)$$

Based on the ω^{-2} model *M(f)* is represented as

$$M(f) = \frac{(2\pi f)^2 M_0}{1 + \left(\frac{f}{f_0}\right)^2}, \quad (2)$$

where M_0 is the seismic moment and f_0 is the corner frequency. The high-cut filter *P(f)* is represented as

$$P(f) = \left(1 + \left(\frac{f}{f_{\max}}\right)^m\right)^{-1/2}, \quad (3)$$

where m is set to be 4.2 [Satoh et al., 1997]. $P(f)$ has a nearly f^{-2} (or ω^{-2}) decay for frequencies below *fmax*. The anelastic attenuation function *T(f)* is represented as

$$T(f) = \exp\left(\frac{-\pi f X}{Q\beta}\right), \quad (4)$$

where X is hypocentral distance. We assume S-wave velocity of β=4.0 km/s [Takemura et al., 1992; Satoh et al., 1997]. We use $Q=110f^{0.69}$ determined by Satoh et al. [1997] because $Q=110f^{0.69}$ is consistent with other previous results estimated from strong motion records around the region interested in this study especially in the frequency higher than 10 Hz as shown by Satoh et al.[1997]. The scaling factor C is given by

$$C = \frac{R_{\theta\phi} FS \cdot PRTITN}{4\pi\rho\beta^3}, \quad (5)$$

where $R_{\theta\phi}$ is the radiation coefficient, *FS* is the amplification factor due to the free surface, *PRTITN* is the reduction factor that accounts for the partitioning of energy into two horizontal components, and ρ is the density of a source region. *FS* is 1.0 and *PRTITN* is taken as $1/2^{1/2}$. It is assumed that $R_{\theta\phi}$ is 0.63 as the average value [Boore and Boatwright, 1984] and ρ is 3.0 g/cm^3 [Takemura et al., 1993; Satoh et al., 1997]. $Z(f)$ is the site amplification factor at GL-330 m in Iwaki and is assumed to be 1.0 as an initial value.

We estimate f_0 and *fmax* for all the 50 earthquakes and M_0 for relatively small 28 earthquakes whose Harvard CMT solutions are not determined. The parameters $\{\boldsymbol{r}\}$(= f_0, *fmax*, and M_0) are estimated to minimize

$$J(\{\boldsymbol{r}\}) = \sum_{j=1}^{2} \int_{fs_{ij}}^{fe_{ij}} \log\left(\frac{O_{ij}(f)}{A(f)} \right) df , \tag{6}$$

where $O_{ij}(f)$ is the acceleration spectrum for the ith earthquake observed at the jth site. Between fs_{ij} and fe_{ij} the signal-to-noise ratio for $O_{ij}(f)$ is greater than three. The quasi-Newton method [Fletcher, 1972] is applied to estimate the parameters, so it is necessary to set initial values for all the parameters. The initial values of M_0 are determined from M_J using M_0-M_J relation proposed by Sato [1979] and the initial values of f_0 are determined from M_0 using M_0-f_0 relation proposed by Satoh et al. [1997]. The initial values of *fmax* are assumed to be 13.5 Hz [Satoh et al., 1997]. After estimating f_0, *fmax*, and M_0 by equation (6), we estimate $Z(f)$ by

$$Z(f) = \frac{1}{2l} \sum_{i=1}^{l} \sum_{j=1}^{2} \frac{O_{ij}(f)}{A(f)} , \tag{7}$$

where $2l$ is the number of the observed spectra. Using the estimated $Z(f)$ we get final values of f_0, *fmax*, and M_0 by equation (6). Stress drop $\Delta\sigma$ is calculated from M_0 and f_0 using the following equation [Brune, 1970].

$$\Delta\sigma = M_0 (f_0/(4.9 \infty 10^6 \beta)^3 , \tag{8}$$

with β in km/s, $\Delta\sigma$ in bars, and M_0 in dyne-cm.

RESULTS

Figure 3(a) shows the amplification factor at GL-330 m in Iwaki, $Z(f)$, obtained from equation (7). Figure 3(b) shows the amplification factor at GL-950 m in Tomioka, which is given as the product of $Z(f)$ shown in Figure 3(a) and the spectral ratio shown in Figure 2. Both of the amplification factors are consistent with theoretical ones based on the one-dimensional wave propagation theory obtained by Kato et al. [1992]. Figure 4 shows the observed spectra corrected by the estimated amplification factors and the model spectra for EQ214 with M_J=5.3 in the region-B. The observed spectra are explained well by the model spectra.

The estimated parameters are listed in Table 1. The estimated *fmax* mostly range from 10 to 20 Hz. Although the parameters in Table 1 are obtained after correcting observed spectra by $Z(f)$ of equation (7), the differences of the estimated values before and after correction are quite small, because $Z(f)$ has a value near unity as shown in Figure 3 (a). Since many earthquakes swarm in the region-A, -B, and -C, first we examine the parameters of earthquakes in the three regions. The relation between *fmax* and M_0 and the relation between *fmax* and $\Delta\sigma$ are shown in Figure 5. We cannot see the significant correlation between M_0 and *fmax*, though it has been suggested in several previous studies (e.g., Faccioli, 1986) that *fmax* decreases with M_0. By contrast, it is found that $\Delta\sigma$ has good correlation with *fmax*. We obtain the following regression relation between $\Delta\sigma$ and *fmax*.

$$\log \Delta\sigma = -2.91 \log fmax + 5.8 \qquad (\sigma=0.296 \text{ ; } \sigma \text{ is standard deviation}) \tag{9}$$

Through a test of significance for the regression coefficients at a 95 % confidence level assuming the *t*-distribution, we confirm that the dependence of *fmax* on $\Delta\sigma$ is significant. In this relation $\Delta\sigma$ is nearly proportional to $fmax^{-3}$, so *fmax* decreases with $\Delta\sigma$. There are no clear differences of *fmax*-M_0 relations and *fmax*-$\Delta\sigma$ relations among the region-A, -B, and -C.

In Figure 6 we show relations between four pairs of parameters estimated for all the earthquakes. We cannot see the significant correlation between *fmax* and M_0. For the relation between *fmax* and $\Delta\sigma$ it is found that the relation in the region-N is consistent with the regression relation obtained from data in the region-A, -B, and -C. Although $\Delta\sigma$ in the region-M is larger than that in the other regions, the relative tendency between $\Delta\sigma$ and *fmax* can be explained by the same gradient of the regression relation. In the region-S, $\Delta\sigma$ is smaller than that in the other regions and the relative tendency between $\Delta\sigma$ and *fmax* is similar to the regression relation. The region-S almost corresponds to the area where Takemura et al. [1989] pointed out that low-frequency earthquakes occur as shown the north boudary by a line in Figure 1. The differences of $\Delta\sigma$ among regions are also seen in the relation between f_0 and M_0. It is reasonable that f_0-M_0 relations in the region-A, -B, -C and -N agree well with the

regression relations obtained by Satoh et al. [1997] and Takemura et al. [1993], because source regions of the data used in the two previous studies are mostly common to the region-A, -B, -C and -N. It is confirmed that M_0 is proportional to f_0^{-3} in the same region except for a few smaller earthquakes with M_0 ♠ $2\infty10^{22}$ dyne-cm. The reason of this deviation of the smaller earthquakes from the others may be low resolution of f_0 and *fmax*, because f_0 tends to decrease and approach to *fmax* as M_0 increases. The relation between M_0 and M_J in this study agree better with Satoh et al.'s relation (1997) rather than Sato's relation (1979). This is consistent with the fact that $\Delta\sigma$ for earthquakes used in this study are almost the same as those for earthquakes used by Satoh et al., but larger than average $\Delta\sigma$ of 50 bar obtained from earthquakes occurred in whole Japan by Sato.

Figure 7 shows *fmax* and $\Delta\sigma$ estimated from shallow borehole records for subduction earthquakes occurred in latitude 37^{o} N to 40^{o} N by Satoh et al. [1997] together with those estimated in this study for earthquakes occurred in the region-A, -B, -C, and -N. This figure suggests that the regression relation in this study is appreciable to subduction earthquakes occurred in latitude 37^{o} N to 40^{o} N, such as off Sanriku earthquakes, off Miyagi prefecture earthquakes as well as off Fukushima prefecture earthquakes.

Finally we discuss the scaling law of acceleration source spectra in the high-frequency range by using the regression relation of equation (9). In the frequencies $f >> fmax$ ε f_0, $M(f)P(f)$ can be approximated from the equations (2) and (3) as follows :

$$M(f)P(f) = (2\pi f_0)^2 M_0 \left(\frac{f_{\max}}{f} \right)^2 \tag{10}$$

Since equation (9) means that $\Delta\sigma$ is nearly proportional to $fmax^{-3}$, we can derive the following relation using the equations (8) and (9) for earthquakes with the same M_0.

$$f_{\max} \propto f_0^{-1}. \tag{11}$$

By using equation (11) that *fmax* is inversely proportional to f_0, equation (10) can be replaced as

$$M(f)P(f) \propto \frac{M_0}{f^2}. \tag{12}$$

From equation (12) it is found that spectral level in the frequency range higher than *fmax* is independent on $\Delta\sigma$ and is dependent on only M_0. As an example in Figure 8 we show $M(f)P(f)$ for an earthquake with $M_0=2.34\infty10^{25}$dyne-cm which is equivalent to $M_J=6.0$ in the M_0-M_J relation proposed by Satoh et al. [1997]. It is confirmed that high-frequency spectral level in the frequencies $f >> fmax$ is scaled by only M_0 in the same source region. The equation (9) suggests that *fmax* is source-controlled. However, the empirical relation cannot be explained by an previous idea that *fmax* is inversely proportional to size of breakdown zone which is assumed to exist just behind the crack tip [e.g., Papageorgiou and Aki, 1983]. Campillo [1983] proposed an another idea that *fmax* is associated with inverse of deceleration time of the rupture front. If we try to interpret the *fmax*-$\Delta\sigma$ relation in this study by the Campillo's idea, it means that deceleration time increases with $\Delta\sigma$, though we cannot show such evidences. We need to interpret the empirical relation further and construct a physical model as the next step.

CONCLUSIONS

Using horizontal components of strong motion records for 50 earthquakes observed by accelerometers installed at GL-330 m in Iwaki and at GL-950 m in Tomioka, Japan, we estimate *fmax* and stress drop $\Delta\sigma$, both of which are key parameters to evaluate high-frequency spectra of strong motions, to fit observed spectrum to the model spectrum based on ω^{-2} model [Boore, 1983]. The conclusions derived from the estimated parameters are summarized as follows:

1. The estimated *fmax* has no correlation with seismic moment M_0.

2. We obtained the following regression relation using strong motion records of 30 earthquakes occurred off Fukushima prefecture (region-A, -B, and -C) in latitude about 37^{o} N.

   $\log \Delta\sigma = -2.91 \log fmax + 5.8$ (σ=0.296 ; σ is standard deviation)

   This empirical relation suggests that *fmax* is source-controlled.

3. The relation that $\Delta\sigma$ is nearly proportional to $fmax^{-3}$ is appreciable to earthquakes occurred in the other three source regions nearby the region-A, -B, and -C, although the level of $\Delta\sigma$ varies with source regions.

4. The regression relation in the above equation can also explain the *fmax*-$\Delta\sigma$ distributions estimated from subduction earthquakes occurred in latitude 37 ^{o} N to 40 ^{o} N in a previous study [Satoh et al., 1997].

5. By substituting the regression relation into acceleration source spectral model, we show that the spectral amplitudes in the frequency range higher than *fmax* is independent on $\Delta\sigma$ and is scaled by only M_0. In other word this scaling law suggests that *fmax* is inversely proportional to f_0 for earthquakes with the same M_0.

ACKNOWLEDGMENT

Strong motion records used in this study are obtained from ten electric power companies in Japan.

REFERENCES

Boore, D. M. (1983), "Stochastic simulation of high-frequency ground motions based on seismological models of the radiated spectra", *Bull. Seism. Soc. Am.*, Vol.73, pp1865-189.

Boore, D. M. and Boatwright J. (1984), "Average body-wave radiation coefficient", *Bull. Seism. Soc. Am.*, Vol.74, pp1615-1628.

Brune, J. N. (1970), "Tectonic stress and the spectra of seismic shear waves from earthquake", *J. Geophys. Res.*, Vol.75, pp4997-5009.

Campillo, M. (1983), "Numerical evaluation of near-field, high-frequency radiation from quasi-dynamic circular faults", *Bull. Seism. Soc. Am.*, Vol.73, pp723-734.

Dziewonski, A. M., Chou, T. A. and Woodhouse, J. H. (1981), "Determination of earthquake source parameters from waveform data for studies of global and regional seismicity", *J. Geophy. Res.*, Vol.86, pp2825-2853.

Faccioli, E. (1986), "A study of strong motions from Italy and Yugoslavia in terms of gross source properties", *Geophys. Monograph*, Vol.37, Maurice Ewing, AGU, 6, pp297-309.

Fletcher, R. (1972), *FORTRAN subroutines for minimization by quasi-Newton methods*, Report R7125 AERE, Harwell, England.

Hanks, T. C. (1982), "fmax", *Bull. Seism. Soc. Am.*, Vol.71, pp1867-1879.

Hauksson, E., Teng, T. and Henyey, T. L. (1987), "Results from a 1500m deep, three-level downholes seismometer array: Site response, low Q values, and fmax", *Bull. Seism. Soc. Am.*, Vol.77, pp1883-1904.

Kato, K., Takemura, M., Ikeura, T., Urao, K. and Uetake, T. (1992), "Preliminary analysis for evaluation of local site effects from strong motion spectra by an inversion method", *J. Phys. Earth*, Vol.40, pp175-191.

Kinoshita, S. (1992), "Local characteristics of the fmax of bedrock motion in the Tokyo metropolitan area, Japan", *J. Phys. Earth*, Vol.40, pp487-515.

Omote, S., Osawa, Y., Ohmura, B., Iizuka, S., Ohta, T. and Takahashi, K. (1984), "Observation of earthquake strong motion with deep boreholes", *Proc. 8th World Conf. Earthq. Eng.*, Vol.2, pp247-254.

Papageorgiou, A. S. and Aki, K. (1983), "A specific barrier model for the quantitative description of inhomogeneous faulting and the prediction of strong ground motion. I. Description of the model", *Bull. Seism. Soc. Am.*, Vol.73, pp693-722.

Sato, R. (1979), "Theoretical basis on relationships between focal parameter and earthquake magnitude", *J. Phys. Earth*, Vol.27, pp353-372.

Satoh, T., Kawase, H. and Sato, T. (1997), "Statistical spectral model of earthquakes in the eastern Tohoku district, Japan based on the surface and borehole records observed in Sendai", *Bull. Seism. Soc. Am.*, Vol.87, pp446-462.

Satoh, T., Kawase, H. and Matsushima, S. (1998). "Source spectra, attenuation function, and site amplification factors estimated from the K-NET records for the earthquakes in the border of Akita and Miyagi prefectures in August, 1996", *Zisin* (*Journal of the Seismological Society of Japan*), Vol.50, pp415-429 (in Japanese with English abstract).

Takemura, M., Hiehata, S., Ikeura, T. and Uetake, T. (1989). "Regional variation of source properties for middle earthquakes in a subduction region", *Zisin* (*Journal of the Seismological Society of Japan*), Vol.42, pp349-359 (in Japanese with English abstract).

Takemura, M., Ikeura, T. and Uetake, T. (1993). "Characteristics of source spectra of moderate earthquakes in a subduction zone along the pacific coast of the southern Tohoku district", *J. Phys. Earth*, Vol.41, pp1-19.

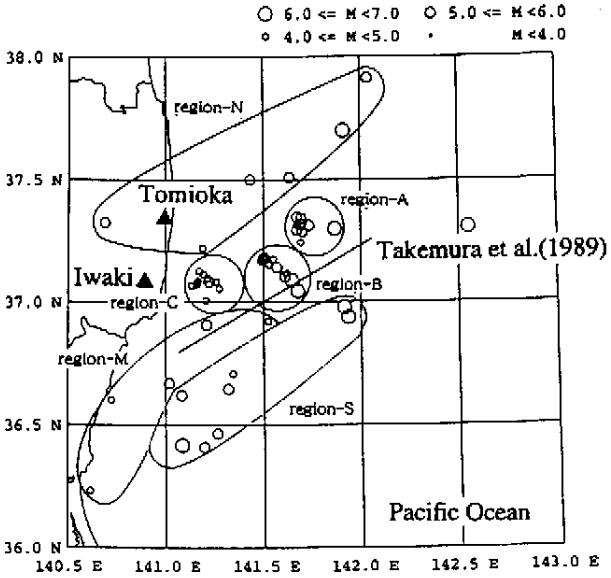

Figure 1 Map of earthquake epicenters and two deep borehole sites

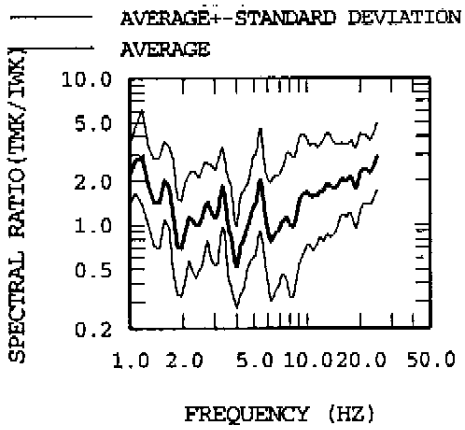

Figure 2 Spectral ratios of Tomioka to Iwaki

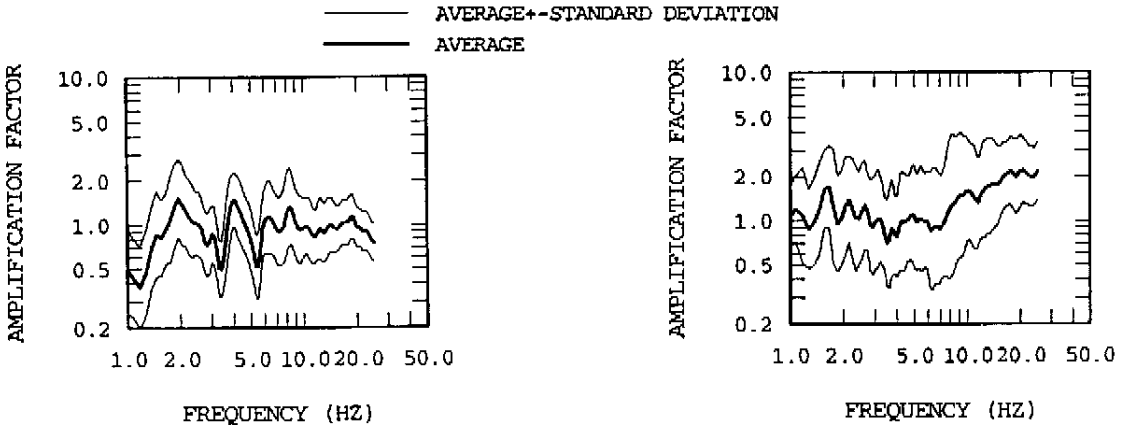

(a) GL-330 m in Iwaki

(b) GL-950 m in Tomioka

Figure 3 Site amplification factors

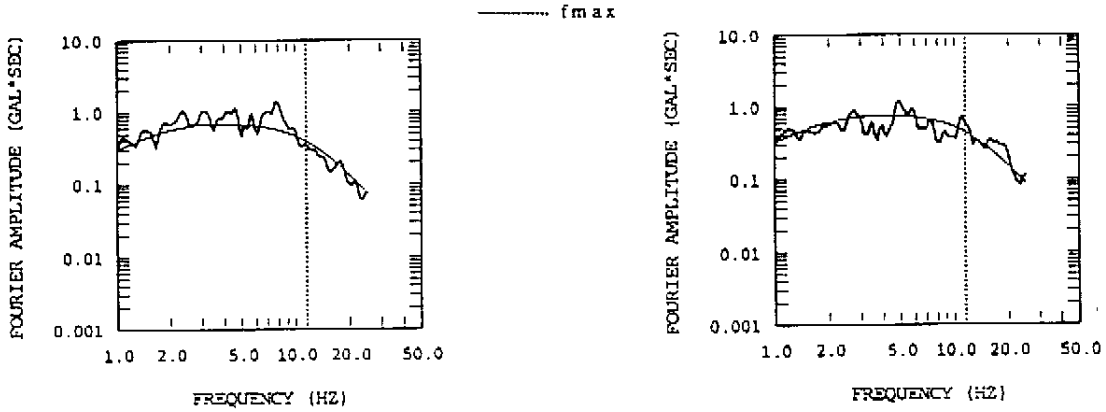

(a) GL-330 m in Iwaki

(b) GL-950 m in Tomioka

Figure 4 Observed acceleration spectra and the fitted model spectra

Table 1 List of parameters estimated for 50 earthquakes

source region	earthquake	estimated parameters			
		M_0 (dyne-cm)	f_0 (Hz)	$\Delta\sigma$ (bar)	f_{max} (Hz)
A	EQ136	3.802×10^{23}	1.64	224.4	13.1
	EQ142	6.607×10^{22}	2.34	111.7	16.5
	EQ147	*1.136×10^{24}*	0.78	72.7	19.1
	EQ163	*5.800×10^{23}*	1.47	246.2	13.8
	EQ188	8.913×10^{22}	4.70	1228.0	15.1
	EQ273	*1.142×10^{26}*	0.32	510.6	10.6
	EQ278	5.888×10^{22}	3.65	380.9	11.9
	EQ287	*3.550×10^{24}*	1.13	685.7	13.3
	EQ318	*2.140×10^{24}*	0.73	112.6	16.0
B	EQ187	4.169×10^{22}	3.41	218.8	11.6
	EQ193	1.023×10^{23}	2.37	180.7	14.8
	EQ200	*7.710×10^{23}*	1.61	428.9	11.7
	EQ201	5.370×10^{22}	3.66	348.3	12.4
	EQ214	*7.760×10^{23}*	1.63	443.9	11.5
	EQ260	2.818×10^{22}	4.58	359.4	12.8
	EQ275	*1.418×10^{25}*	0.32	64.2	22.7
	EQ277	*1.081×10^{26}*	0.25	226.5	14.5
	EQ280	1.549×10^{23}	2.39	282.2	11.2
	EQ281	1.905×10^{23}	2.39	343.3	15.3
C	EQ91	2.512×10^{23}	2.57	566.3	14.1
	EQ156	1.549×10^{22}	5.02	260.4	14.1
	EQ160	2.570×10^{23}	1.75	182.0	13.3
	EQ161	8.128×10^{22}	4.21	806.1	7.3
	EQ168	1.514×10^{22}	6.57	569.8	12.2
	EQ218	1.950×10^{22}	8.15	1402.0	12.8
	EQ219	3.090×10^{23}	1.19	69.7	16.9
	EQ255	*2.980×10^{24}*	0.93	318.9	12.5
	EQ284	1.905×10^{23}	1.34	61.0	19.0
	EQ481	2.291×10^{23}	1.49	99.8	18.4
	EQ515	1.950×10^{22}	10.18	2732.0	12.1

source region	earthquake	estimated parameters			
		M_0 (dyne-cm)	f_0 (Hz)	$\Delta\sigma$ (bar)	f_{max} (Hz)
N	EQ95	7.943×10^{23}	0.99	103.0	17.0
	EQ132	*1.740×10^{24}*	0.89	162.9	13.4
	EQ167	*4.590×10^{23}*	1.84	379.8	11.3
	EQ199	2.454×10^{22}	3.10	97.0	25.1
	EQ220	*1.190×10^{24}*	1.68	753.4	11.3
	EQ223	*5.750×10^{25}*	0.30	199.9	13.6
M	EQ106	4.074×10^{22}	6.43	1441.0	18.7
	EQ134	*3.450×10^{24}*	0.93	363.5	22.0
	EQ140	2.512×10^{23}	2.28	394.4	18.3
	EQ239	2.630×10^{23}	1.96	264.2	23.3
	EQ247	1.445×10^{23}	4.82	2150.0	10.2
S	EQ139	1.230×10^{23}	2.03	135.9	8.8
	EQ154	*2.590×10^{24}*	0.54	54.9	11.0
	EQ236	*2.480×10^{25}*	0.23	42.2	12.7
	EQ262	*6.530×10^{24}*	0.40	56.5	13.7
	EQ267	*4.360×10^{25}*	0.21	50.1	16.0
	EQ268	*1.320×10^{26}*	0.18	97.9	16.0
	EQ269	2.951×10^{24}	0.66	113.2	14.2
	EQ286	*7.780×10^{24}*	0.42	75.1	13.7
-	EQ528	*1.329×10^{26}*	0.42	1308.0	17.2

Mo in Italic is Harvard CMT solution

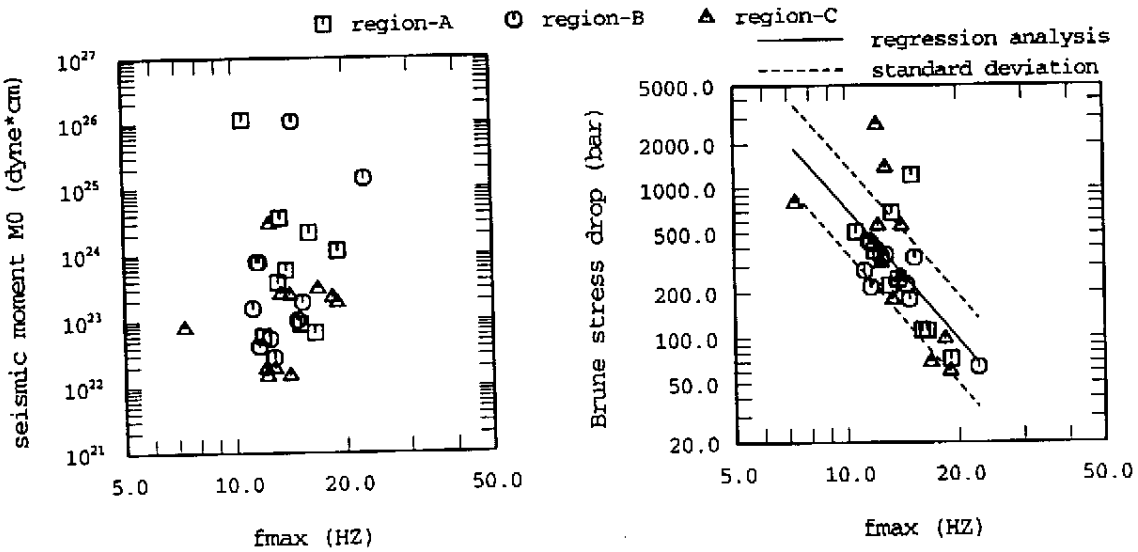

Figure 5 Relations between parameters for earthquakes in the region-A, -B, and -C

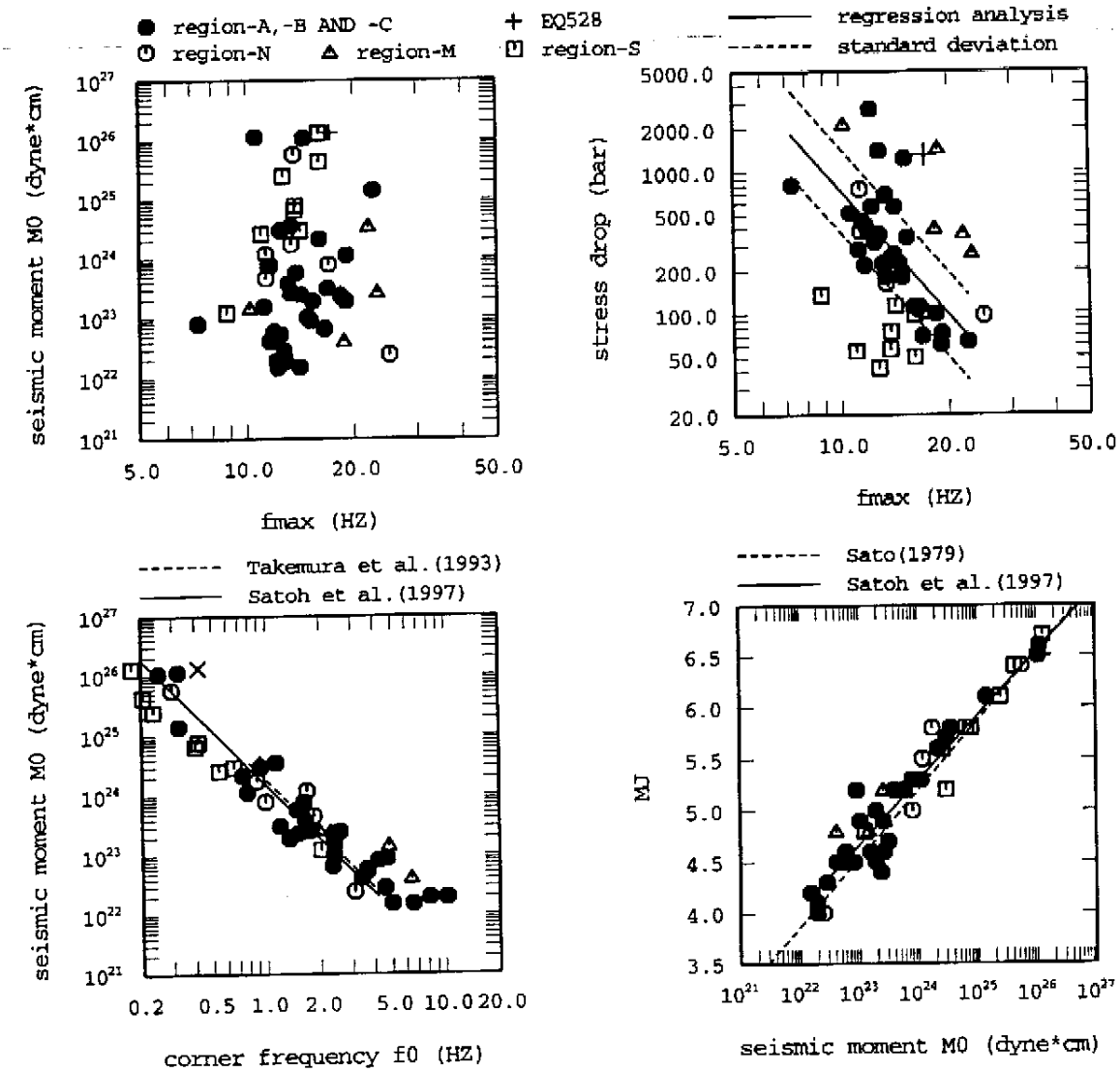

Figure 6 Relations between parameters for all the earthquakes

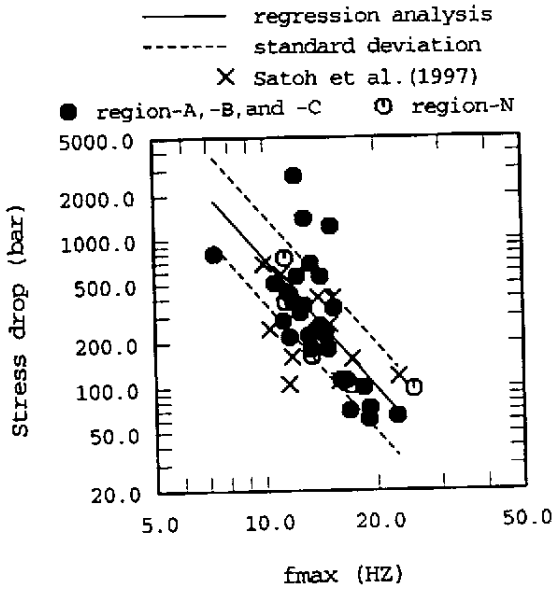

Figure 7 Relations between *fmax* and $\Delta\sigma$ for earthquakes used in this study and Satoh et al.'s

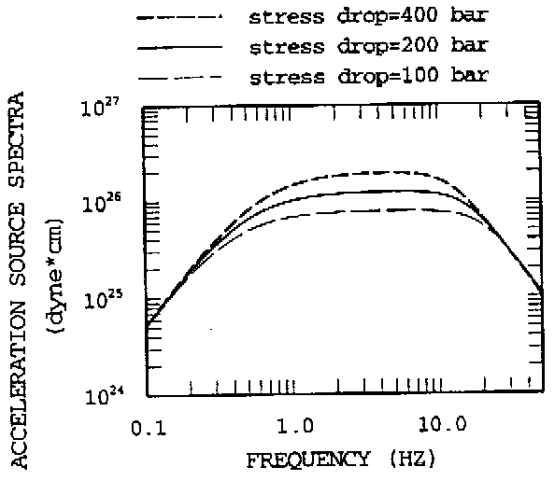

Figure 8 Acceleration source spectral model $M(f)P(f)$ for an earthquake with M_0=2.34×10^{25}dyne-cm (M_J=6.0)